# Modeling of the Methyl Methacrylate Atom Transfer Radical Suspension Polymerization Process: Polymerization and Particle Kinetics

Le Xie, Zheng-Hong Luo*

In this work, a mathematical model is developed to characterize the batch atom transfer radical suspension polymerization (batch suspension ATRP). For the first time, the morphological and molecular properties of particles, as well as their dynamics in methyl methacrylate ATRP can be simultaneously simulated by solving the model that consists of ATRP kinetic equations, moment equations, a phase equilibrium equation for calculating equilibrium monomer distributions in various phases, and a particle population balance model. The proposed model is verified using the open experimental data. Based on the verified model, two key operating factors including the ratios of monomer to initiator and water to monomer are studied in order to investigate the batch suspension ATRP kinetics. In addition, the model is also used to predict the droplet/particle size distribution. The effects of breakage rate, coalescence rate, and agitation speed on the droplet volume density distribution and the Sauter mean diameter are discussed in details. The simulated results demonstrate that the coupled model can describe the batch suspension ATRP kinetics and its droplet kinetics.
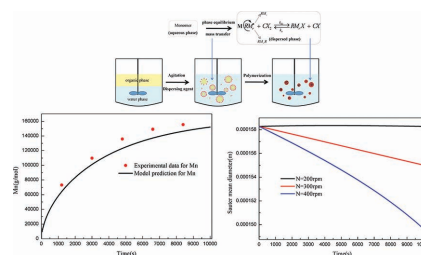
1. Introduction

During the past 20 years, there was much progress in the atom transfer radical polymerization (ATRP) field. The past progress focused on ATRP mechanism, kinetics, and methodology.[1–6] Besides, the ATRP technology has already been commercialized in USA and Japan, etc.[7] Nevertheless, past ATRPs were mostly implemented in organic solution, bulk, and emulsion.[8–10] Few studies on suspension ATRP have been reported.[11–14]

Due to its huge advantages in avoiding the two main problems (i.e., the highly exothermic reactions, the large

Dr. L. Xie, Prof. Z.-H. Luo
Department of Chemical Engineering
College of Chemistry and Chemical Engineering
Shanghai Jiao Tong University
Shanghai 200240, P. R. China
E-mail: luozh@sjtu.edu.cn

increase in viscosity),[15] suspension polymerization is one of the most important technologies applied in the polymerization industry. A key consideration in designing a suspension polymerization is to achieve such that desired molecular microstructure and droplet/particle size distribution (PSD) of polymers are satisfied. The number average molecular weight (M_n) and polydispersity index (PDI), as the most basic performance indices of polymer affecting the polymer end-use properties, are mainly determined by polymerization kinetics, and the PSD can control some key aspects of operation including suspension stability and productivity. Hence, there is a growing demand for studying suspension polymerization kinetics and its droplet/particle kinetics.

For a suspension polymerization, two characteristic phases, i.e., the aqueous phase and the dispersed phase, are present. If the dissolved monomer in the aqueous phase is ignored, the polymerization process occurring at the suspension droplets will be considered as a bulk one.

Early View Publication; these are NOT the final page numbers, use DOI for citation !!

Based on this opinion, Kalfas et al.[16] developed a two-phase free-radical kinetic model for suspension polymerization. Their simulated results were in good agreement with batch suspension experimental data when using kinetic parameters from the bulk polymerization literatures. Similar works of vinyl chloride and styrene copolymerization kinetics in bulk and suspension polymerizations were also found in the open literature.[17] When monomers partially dissolve in the aqueous phase, the mass transfer phenomena between the aqueous phase and the dispersed phase would affect the whole suspension polymerization process, which makes the process more complex.[18] Kalfas and Ray[19] put foward a mathematical model to describe the suspension polymerization of partially water-soluble monomers. Their simulated results were consistent with the experimental data from both the literature and their suspension polymerization experiments. To describe the dynamic conversion and molecular weight profiles of suspension polymerization, Silva et al.[20] performed a detailed research considering the monomer partition between the aqueous and organic phases for vinyl acetate/acrylic acid suspension copolymerization. Successful descriptions of the large variations of copolymer compositions along the reaction runs were obtained. Wieme et al.[21] also developed a complete model to simulate pilot-scale and industrial-scale batch vinyl chloride suspension polymerization reactors. As a whole, the above models can provide quantitative agreement with limited experimental data. Unfortunately, the previous studies mainly focused on traditional free radical polymerization system. Less effort paid to the suspension ATRP. The kinetic behavior of the suspension ATRP of MMA at different temperatures was investigated by Zhu et al.[13] However, the dynamic behavior of the partitioning of the monomer over the two phases was not considered in their work.

On the other hand, in the suspension polymerization field, there are many publications on PSD based on the population balance model (PBM). For instance, Vivaldo-Lima et al.[22] presented a comprehensive review providing detailed information on the development of theoretical model to predict the PSD in suspension polymerization. Maggioris et al.[23] studied the effect of turbulence nonhomogeneity on the evolution of PSD in vinyl chloride suspension polymerizations based on a two-compartment PBM. They investigated broad spatial distribution of the local turbulent kinetic energy. Similarly, Kotoulas and Kiparissides[24] proposed a generalized PBM to describe the dynamic evolution of PSD in nonreactive and reactive liquid (solid)–liquid suspension polymerization systems. Their predicted data were in line with the experimental data for the average particle diameter and PSD. Recently, Nogueira et al.[25] evaluated the spatial distribution of droplet breakage and droplet coalescence based on the

multiphase computational fluid dynamics (CFD) models for the first time. According to their simulated results, particle breakage occurred primarily in very small regions near the impeller, while particle coalescence took place in the liquid bulk. However, the polymerization reaction kinetics was ignored in their model. Bárkányi et al.[26] coupled the PBM with micromixing model to simulate an isothermal batch suspension polymerization, thus a complex three-scale system model was developed to investigate the effect of coalescence, breakage, and micromixing on the process. In conclusion, as described above, both reaction kinetics and particle kinetics are very important for suspension polymerization, especially for consideration of products performance.

The current work proposes a coupled model describing the polymerization kinetics and the evolution of PSD in a batch suspension ATRP reactor. For the first time, the ATRP kinetic equations are solved using the method of moment in the polymerization engineering field, the phase equilibrium equation, the constitutive equations of dispersed phase, and the PBMs. The time evolutions of polymerization conversion, polymer M_n, PDI, and PSD are obtained using the coupled model.

2. Model Developments

2.1. Suspension ATRP Kinetics Model

In this work, it is assumed that both suspension and bulk ATRPs have a similar kinetic mechanism consisting of initiation, propagation, and chain transfer to monomer along with termination reactions as illustrated in Table 1. Furthermore, the ATRP takes place only in the dispersed phase under isothermal conditions. Since MMA partially dissolves in water, we assumed that the phase equilibrium

■ *Table 1.* Elementary Reactions of suspension ATRP.

Initiation	$RX + CX \underset{k_{da,o}}{\overset{k_{a,o}}{\rightleftarrows}} R^{\bullet} + CX_2$
	$R^{\bullet} + M \xrightarrow{k_{in,A}} RM_1^{\bullet}$
Propagation	$RM_rX + CX \underset{k_{da}}{\overset{k_a}{\rightleftarrows}} RM_r^{\bullet} + CX_2$
	$RM_r^{\bullet} + M \xrightarrow{k_p} RM_{r+1}^{\bullet}$
Chain transfer to monomer	$RM_r^{\bullet} + M \xrightarrow{k_{tr}} RM_r + M^{\bullet}$
Termination	$R^{\bullet} + R^{\bullet} \xrightarrow{k_{to}} RR$
	$R^{\bullet} + RM_r^{\bullet} \xrightarrow{k_{tR}} RM_rR$
	$RM_r^{\bullet} + RM_s^{\bullet} \xrightarrow{k_{td}} RM_r + RM_s$
	$RM_r^{\bullet} + RM_s^{\bullet} \xrightarrow{k_{tc}} RM_{r+s}R$

www.MaterialsViews.com

Early View Publication; these are NOT the final page numbers, use DOI for citation !!

Modeling of the Methyl Methacrylate Atom Transfer Radical Suspension Polymerization Process: Polymerization . . .

Macromolecular
Reaction Engineering

www.mre-journal.de

of MMA between two phases forms before the polymerization starts. With the proceeding of polymerization process, the monomer concentration in the dispersed phase decreases, resulting in the mass transfer of monomer from aqueous phase to dispersed phase. Based on the above description, a set of differential equations can be obtained and are given as follows

$$\frac{1}{V}\frac{d(V[RX])}{dt} = -k_{a,o}[RX][CX] + k_{da,o}[R^\bullet][CX_2] \tag{1}$$

$$\frac{1}{V}\frac{d(V[CX])}{dt} = k_{da,o}[R^\bullet][CX_2] - k_{a,o}[RX][CX]$$
$$+ k_{da}[RM_r^\bullet][CX_2] - k_a[RM_rX][CX] \tag{2}$$

$$\frac{1}{V}\frac{d(V[CX_2])}{dt} = -k_{da,o}[R^\bullet][CX_2] + k_{a,o}[RX][CX]$$
$$- k_{da}[RM_r^\bullet][CX_2] + k_a[RM_rX][CX] \tag{3}$$

$$\frac{1}{V}\frac{d(V[R^\bullet])}{dt} = -k_p[M][R^\bullet] - k_{da,o}[R^\bullet][CX_2]$$
$$+ k_{a,o}f[RX][CX] - k_{to}[R^\bullet][R^\bullet] - k_{tR}[R^\bullet][RM_r^\bullet] \tag{4}$$

$$\frac{1}{V}\frac{d(V[RM_r^\bullet])}{dt} = k_p[RM_{r-1}\cdot][M_i] - k_p[RM_r\cdot][M]$$
$$+ k_a[RM_rX][CX] - k_{da}[RM_r\cdot][CX_2]$$
$$- (k_{tc} + k_{td})[RM_r\cdot][RM_s\cdot] - k_{tr}[RM_r\cdot][M]$$
$$- k_{tR}[R^\bullet][RM_r^\bullet] \tag{5}$$

$$\frac{1}{V}\frac{d(V[RM_rX])}{dt} = k_{da}[RM_r\cdot][CX_2] - k_a[RM_rX][CX] \tag{6}$$

$$\frac{1}{V}\frac{d(V[RM_r])}{dt} = k_{td}[RM_r\cdot][RM_s\cdot] + k_{tr}[RM_r\cdot][M] \tag{7}$$

$$\frac{1}{V}\frac{d(V[RM_rR])}{dt} = \frac{1}{2}k_{tc}[RM_{r-s}\cdot][RM_s\cdot] + k_{tR}[R^\bullet][RM_r^\bullet] \tag{8}$$

In these equations, $[M]$ is the monomer, $[RX]$ is the initiator, $[CX]$ is the activator (CuCl), $[CX_2]$ is the deactivator (CuCl$_2$), $[R^\bullet]$ is the primary radical, $[RM_r^\bullet]$ is the propagating radical chain, $[RM_rX]$ is the dormant chain, and $[RM_r]$, $[RM_rR]$ are the dead chains with length r formed by disproportionation and coupling termination, respectively. As described above, the monomer partially dissolves in the aqueous phase, its mass conservation in two phases needs

to be considered. The monomer transport rate will be computed according to Equation (9)

$$F_{a\to d} = k_{ma}([M]^e - [M]) \tag{9}$$

Where, $[M]^e$ is the equilibrium concentration in the dispersed phase which is a function of MMA dissolved in the aqueous phase (mol L^{-1}) and will be explained further below. Therefore, the monomer mass balance in the dispersed phase including monomer transport between the two phases is

$$\frac{1}{V}\frac{d(V[M])}{dt} = -k_p[R^\bullet][M] - (k_p + k_{tr})[RM_r^\bullet][M]$$
$$+ k_{ma}([M]^e - [M]) \tag{10}$$

Then the monomer conversion in the dispersed phase can be defined as follows

$$X_m = \frac{[M]_o V_o - [M]V}{[M]_o V_o} \tag{11}$$

Where, $[M]_0$ and V_0 are the initial conditions for dispersed phase, respectively. Similarly, monomers conservation equation in the aqueous phase is

$$\frac{1}{V_a}\frac{d(V_a[M_a])}{dt} = -k_{ma}([M]^e - [M]) \tag{12}$$

Here, it should be pointed out that the change of aqueous phase volume (V_a) is neglected, while the dispersed phase volume decreases during the polymerization due to the density difference between monomer and polymer. That is to say, the dispersed phase volume is the function of monomer conversion and can be described as follows

$$V = V_o(1 - \psi X_m) \tag{13}$$

Where, ψ is the volume contraction factor and is given by $\psi = (\rho_p - \rho_m)/\rho_p$.

In this paper, the polymerization kinetic equations are rewritten by introducing the method of moment, which was commonly used for modeling various polymerization processes, to simplify the calculation and describe the polymer product properties (i.e., M_n, PDI) more conveniently. For a generalized description of the method of moments, the readers are encouraged to refer to the papers of Zhu and co-workers.[27–29] Herein, only some main equations on the definition of moment are given as follows

$$\mu_m = \sum_{r=1}^{\infty} r^m [RM_r^\bullet], \quad \lambda_m = \sum_{r=1}^{\infty} r^m [RM_rX],$$
$$\omega_m = \sum_{r=1}^{\infty} r^m([RM_rR] + [RM_r]) \tag{14}$$

Materials
Views

www.MaterialsViews.com

Macromol. React. Eng. **2016**, DOI: 10.1002/mren201500074
© 2016 WILEY-VCH Verlag GmbH & Co. KGaA, Weinheim

Macromolecular
Journals

3

Therefore, the moment equations for various species are obtained when Equation (14) is substituted into the polymerization kinetic equations.[30,31] What's more, based on the first few moment equations, the polymer average properties such as number-average chain length (r_n), weight-average chain length (r_w), M_n, M_w, and PDI can be obtained based on the following equations

$$r_n = \frac{\mu_1 + \lambda_1 + \omega_1}{\mu_o + \lambda_o + \omega_o} \tag{15}$$

$$M_n = \frac{\mu_1 + \lambda_1 + \omega_1}{\mu_o + \lambda_o + \omega_o} M_M \tag{16}$$

$$r_w = \frac{\mu_2 + \lambda_2 + \omega_2}{\mu_1 + \lambda_1 + \omega_1} \tag{17}$$

$$M_w = \frac{\mu_2 + \lambda_2 + \omega_2}{\mu_1 + \lambda_1 + \omega_1} M_M \tag{18}$$

$$\text{PDI} = \frac{r_w}{r_n} = \frac{(\mu_2 + \lambda_2 + \omega_2)(\mu_o + \lambda_o + \omega_o)}{(\mu_1 + \lambda_1 + \omega_1)^2} \tag{19}$$

2.2. Calculation of the Equilibrium Concentration

For the above equations, one of the major issues is the calculation of the monomer equilibrium concentration. In this study, the equilibrium concentration is calculated based on the Flory–Huggins lattice theory of polymer solutions.[19,32] Therefore, the free energy of mixing in aqueous and dispersed phase is presented in the following

Aqueous phase (monomer + water) :

$$(\Delta G_m / RT)_{i,a} = \ln(\phi_{i,a}) + (1 - m_{iW})\phi_{W,a} + \chi_{iW}\phi_{W,a}^2$$
$$+ \sum_{j=1, j\neq i}^{N} \phi_{j,a}\phi_{W,a}(\chi_{ij} + \chi_{iW} - \chi_{jW}m_{ij}) + \sum_{j=1}^{N}(1 - m_{ij})\phi_{j,a}$$
$$+ \sum_{j=1, j\neq i}^{N} \chi_{ij}\phi_{j,a}^2 + \sum_{j=1, j\neq i}^{N-1} \sum_{k=j+1, k\neq i}^{N} \phi_{j,a}\phi_{k,a}(\chi_{ij} + \chi_{ik} - \chi_{jk}m_{ij})$$
$$\tag{20}$$

Dispersed phase (monomer + polymer):

$$(\Delta G_m / RT)_{i,d} = \ln(\phi_{i,d}) + (1 - m_{iP})\phi_{P,d} + \chi_{iP}\phi_{P,d}^2$$
$$+ \sum_{j=1, j\neq i}^{N} \phi_{j,d}\phi_{P,d}(\chi_{ij} + \chi_{iP} - \chi_{jP}m_{ij}) + \sum_{j=1}^{N}(1 - m_{ij})\phi_{j,d}$$
$$+ \sum_{j=1, j\neq i}^{N} \chi_{ij}\phi_{j,d}^2 + \sum_{j=1, j\neq i}^{N-1} \sum_{k=j+1, k\neq i}^{N} \phi_{j,d}\phi_{k,d}(\chi_{ij} + \chi_{ik} - \chi_{jk}m_{ij})$$
$$\tag{21}$$

Where, χ_{ij} is the Flory–Huggins interaction parameter of species i and species j, $\varphi_{i,d}$ represents the volume fraction

of species i in phase d, and m_{ij} is the ratio of the molar volumes of species i and species j. When the phase equilibrium is achieved

$$(\Delta G_m / RT)_{i,a} = (\Delta G_m / RT)_{i,d} \tag{22}$$

Then monomer equilibrium concentration, $[M]^e$, can be calculated based on the normalization condition in two phases. Obviously, $[M]^e$ is a function of the amount of monomer dissolved in the aqueous phase. In suspension polymerization, the droplet size is usually greater than 50 µm so that the effect of interfacial tension energy can be neglected, and the presence of water in the dispersed phase is also neglected.[19]

2.3. Particle Kinetic Model

A PBM developed in this study for describing the time evolution of the particles/droplets size distribution of dispersed phase is described as follows[15]

$$\frac{\partial n(v,t)}{\partial t} + \frac{\partial}{\partial v}[G(v)n(v,t)] = E(v,t) - D(v,t) \tag{23}$$

where, $n(v,t)$ is the number density function, $G(v)n(v,t)$ means the particle flux due to particle growth, and $E(v,t)$ and $D(v,t)$ denote birth and death rate functions of breakage and coalescence, respectively. They can be written as follows

$$E(v,t) = \int_v^\infty \beta(u,v)\upsilon(u)s(u)n(u,t)\,du$$
$$+ \int_o^{v/2} \kappa(v-u,u)n(v-u,t)n(u,t)\,du \tag{24}$$

$$D(v,t) = n(v,t)\int_o^\infty \kappa(v,u)n(u,t)\,du + s(v)n(v,t) \tag{25}$$

In Equations (24) and (25), $s(v)$ and $\kappa(v,u)$ is the breakage rate and coalescence rate, respectively. In this work, suspension polymerization is assumed at the inertial subrange, where turbulence affects particle breakage and coalescence significantly. Additionally, the largely increased viscosity will also affect these phenomena. Thus, breakage and coalescence rates are calculated based on frequency and Maxwellian efficiency[33] and the modifications by Chen et al.[15] as follows

$$s(v) = k_b \exp\left(-\frac{k_c \sigma (1+\phi)^2}{\rho_d v^{5/9} \varepsilon^{2/3}} - \frac{k_v \mu_d (1+\phi)}{\rho_d v^{4/9} \varepsilon^{1/3}}\right) \tag{26}$$

$$\kappa(v,u) = \alpha_b \exp\left(-\frac{\alpha_c \mu_d \rho_d \varepsilon}{\sigma^2 (1+\phi)^3}\left(\frac{d_v d_u}{d_v + d_u}\right)^4\right) \tag{27}$$

In addition, the functions, $\upsilon(u)$ and $\beta(u,v)$ represent the number and distribution of daughter droplets formed by

Early View Publication; these are NOT the final page numbers, use DOI for citation !!

Modeling of the Methyl Methacrylate Atom Transfer Radical Suspension Polymerization Process: Polymerization ...

Macromolecular
Reaction Engineering

www.mre-journal.de

■ *Table 2.* Model parameters at 90 °C.

Descriptions	Values	References	Descriptions	Values	References
$k_a, k_{a,0}$(L mol^{-1} s^{-1})	1.2853	[30]	k_c	2.4732×10^{-3}	[15]
$k_d, k_{d,0}$(L mol^{-1} s^{-1})	1.2597×10^6	[30]	k_v	4.1445×10^{-3}	[15]
k_p(L mol^{-1} s^{-1})	1539	[13]	α_b	3.4578×10^{-6}	[15]
k_{tr}(L mol^{-1} s^{-1})	0.0198	[34]	α_c	4.9200×10^{11}	[15]
k_{tc}^0(L mol^{-1} s^{-1})	1.0×10^7	[35]	μ_m (Pa·s)	0.000425	This work
k_{td}^0(L mol^{-1} s^{-1})	8.86×10^7	[35]	ρ_m (kg/m^3)	866	This work
k_{tR}, k_{t0}(L mol^{-1} s^{-1})	2.0×10^9	[36]	ρ_p (kg/m^3)	1095	This work
K_{ma} (1 s^{-1})	2.0×10^{-7}	[19]	χ_{MW}	0.74	[37]
k_b	2.3951×10^{-4}	[15]	χ_{MP}	0.53	[37]

breakage events, respectively. Herein, it is assumed that the daughter droplet size distribution conforms to the normal distribution. Thus, for binary breakage, the droplet rupture functions, $\upsilon(u)$ and $\beta(u,v)$, can be given[23,33]

$$\upsilon(u) = 2\ \beta(u,v) = \frac{2.4}{v}\exp\left(-4.5\frac{(2u-v)^2}{v^2}\right) \qquad (28)$$

Furthermore, the Sauter mean diameter (d_{32}) will be calculated by Equation (29) with the given initial and boundary conditions

$$d_{32} = \frac{(6/\pi)^{1/3}\int_o^\infty v^{1/3}n(v,t)dv}{\int_o^\infty n(v,t)dv} \qquad (29)$$

2.4. Physical Properties of Dispersed Phase

In suspension polymerization, the density and viscosity of the dispersed phase changes with monomer conversion and should have a vital effect on the evolution of PSD according to Equations (26) and (27). In this study, the dispersed phase density is calculated as a function of monomer conversion with the expression

$$\rho_d = [(1-\psi X_m)/\rho_m]^{-1} \qquad (30)$$

To describe the change of viscosity, its dependence on the monomer conversion of the polymerizing Poly(methyl methacrylate) (PMMA) particle is described as below[23]

$$\mu_d = \mu_m[1+1.25X_m\rho_d/\rho_p(1-X_m\rho_d/\rho_p)]^2 \qquad (31)$$

Where, μ_m is the monomer viscosity. Obviously, when the monomer conversion is low, the dispersed phase viscosity is approximately the monomer viscosity.

3. Numerical Simulation

To solve the above-developed model, model parameters, mainly polymerization kinetic and particle kinetic

parameters, need to be confirmed in advance. Herein, these parameters are obtained from some open references and our previous works as shown in Table 2 and the polymerization data were taken from Zhu et al.'s suspension ATRP performed at 90 °C.[13] What is more, the termination rate coefficient is given according to Equation (32)

$$k_t = g_t(k_{tc}^o + k_{td}^o) \qquad (32)$$

where the gel effect coefficient (g_t) is the function of X_m and can be described as below[16]

$$g_t = \exp(-0.4404X_m - 6.362X_m^2 - 0.1704X_m^3) \qquad (33)$$

An initial particle size distribution is also required to solve the population balance equation (PBE). In this study, it is assumed that the initial particle size distribution containing 10^4–10^6 droplets with a mean diameter of 160 μm follows a normal distribution, and the variance that is three times as much as the mean volume is adopted.

The polymerization kinetic model consists of a set of differential moment equations, while particle kinetic model is a nonlinear integro-differential equation. A large amount of computation effort is required to solve the two kinetic models simultaneously. Chen et al.[15] reported a finite-difference-differential technique and a logarithmic scale for particle size, so that the PBM is changed into a set of ordinary differential equations. The ODE23S-function provided in MATLAB 2012b (8.0) software can be used to solve the differential equations to obtain X_m, M_n, PDI, and PSD.

4. Results and Discussion

4.1. Validation of the Coupled Model

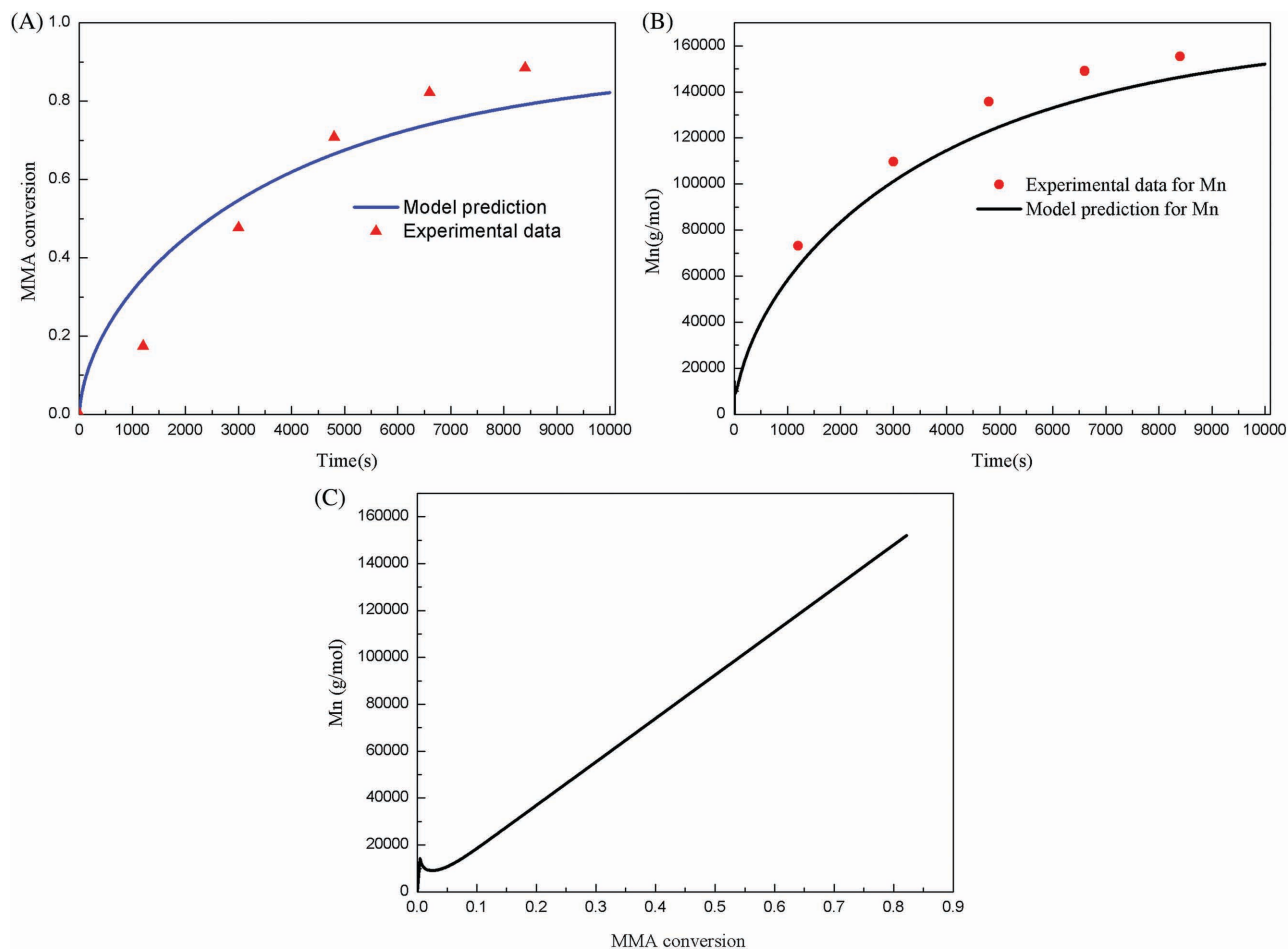In this study, the batch suspension ATRP experimental data reported by Zhu et al.[13] are used to validate the

Materials
Views

www.MaterialsViews.com

Macromol. React. Eng. **2016**, DOI: 10.1002/mren201500074
© 2016 WILEY-VCH Verlag GmbH & Co. KGaA, Weinheim

Macromolecular
Journals

5

Figure 1. Comparisons between simulation results and experimental data[13] for the batch suspension ATRP at 90 °C: A) monomer conversion versus time and B) PDI and M_n versus time. Simulation and experimental conditions: $[MMA]_o = 9.36$ mol L^{-1}; $[RX]_o = 0.047$ mol L^{-1}; $[CuCl]_o = 0.047$ mol L^{-1}; $[bpy]_o = 0.14$ mol L^{-1}; M/W = 1:4.

present model. It is well-known that monomer conversion, M_n, and PDI were the main important polymer properties in the description of polymerization process. Figure 1A shows the evolution of monomer conversion during the polymerization. As the polymerization proceeds, the MMA conversion finally increases to 82%, which is slightly less than that of MMA bulk polymerization and the experimental data reported by Zhu et al.[13] The monomer concentration distribution in two phases could be one of the most important reasons. Even so, the simulated monomer conversion data are consistent with the experimental data. Besides, some experimental data of polymer properties are also used to test the coupled model. Figure 1B displays the evolution of M_n with polymerization time. As can be seen clearly, the M_n increases to 1.5×10^5 g mol^{-1} in the reaction time of 10 000 s. The polymer M_n is much higher than the theoretical value under the specified initial condition. Zhu et al.[13] explained that the low initiator efficiency would be one of the main reasons. According to the reported experimental data, a low initiator efficiency

value $f = 0.11$ is used in our simulations (see Equation (4)). In addition, Figure 1C shows the variation of polymer M_n with monomer conversion. As can be seen, the polymer M_n increases almost linearly with monomer conversion, indicating that the suspension polymerization is basically at a controlling fashion. The particle size may be another important factor in suspension polymerization for liquid–liquid disperse system, and the average particle size in batch reactor can be calculated according to the classic equation found elsewhere.[38,39] In this work, however, the Sauter mean diameter is calculated based on the initial distribution that is determined by ourselves. What's more, little experimental data could be obtained to compare with the simulation results so that the validation of the particle population balance model may have many difficulties. In conclusion, Figure 1 shows that the simulated results are in agreement with the reported experimental data. Accordingly, the suggested model can be used to simulate the effects of other factors, which will be discussed in Sections 4.2 and 4.3.
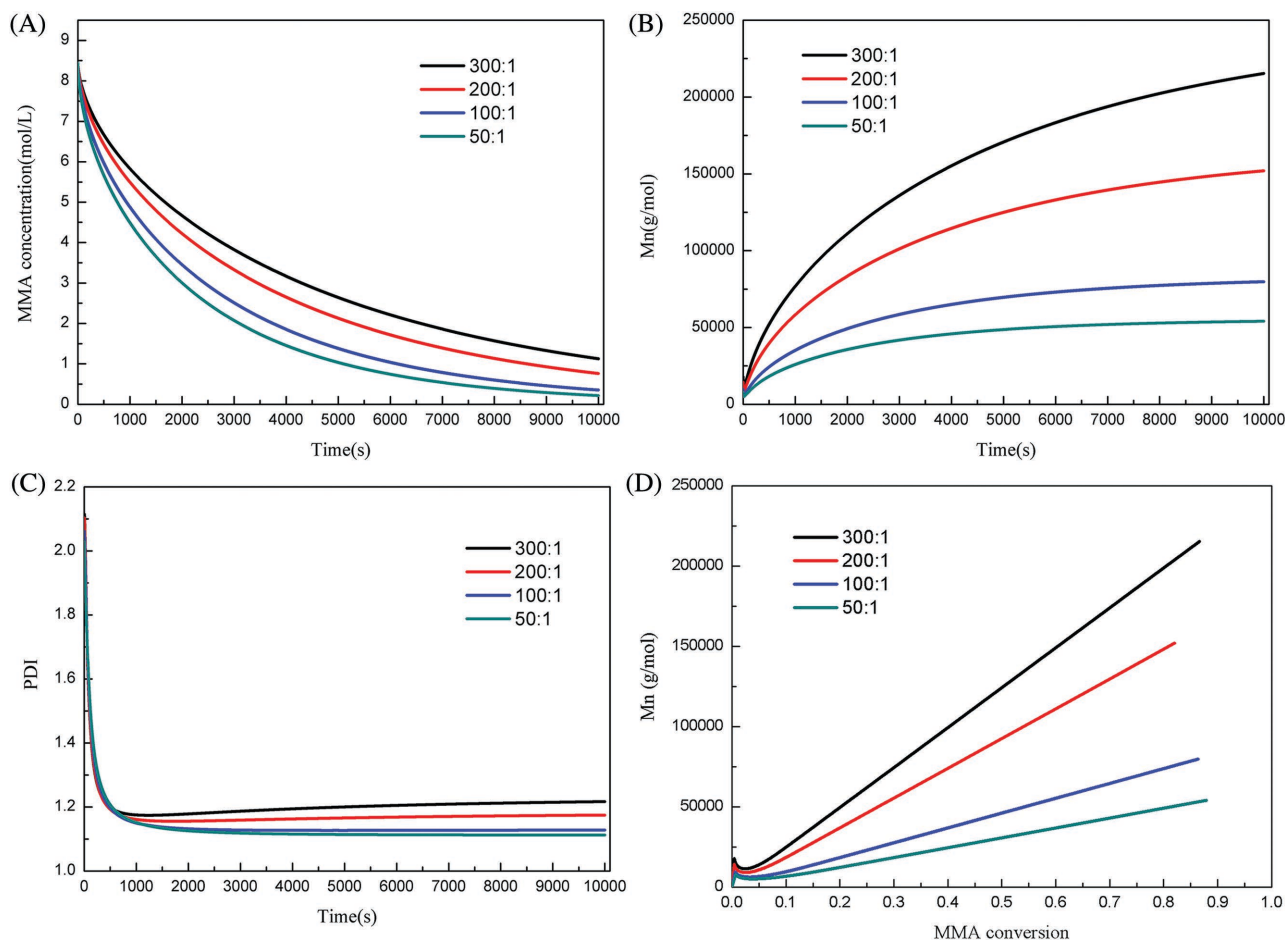
Early View Publication; these are NOT the final page numbers, use DOI for citation !!

Modeling of the Methyl Methacrylate Atom Transfer Radical Suspension Polymerization Process: Polymerization . . .

Macromolecular
Reaction Engineering

www.mre-journal.de

Figure 2. Simulation results of batch suspension ATRP process at four monomer/initiator ratios: A) monomer concentration versus time, B) M_n versus time, C) PDI versus time. MMA suspension polymerization at 90 °C and $[MMA]_o = 9.36$ mol L^{-1}; $[CuCl]_o = 0.047$ mol L^{-1}; $[bpy]_o = 0.14$ mol L^{-1}; M/W = 1:4.

4.2. The Suspension ATRP Kinetics

4.2.1. The Effect of the Ratio of Monomer to Initiator

It is well-known that the polymerization kinetics is much influenced by the polymerization recipe such as the initial monomer concentration, initiator concentration, etc. These parameters can also affect the final polymer properties, and therefore receive quite a lot of attention. In this section, we mainly studied the effect of monomer/initiator ratio on suspension polymerization process along with polymer properties. The simulated results shown in Figure 2A–D illustrate the evolutions of these properties when the initial monomer/initiator ratio changes from 50:1 to 300:1. As can be seen from Figure 2, the monomer/initiator ratio has significant effect on the monomer conversion, polymer M_n, and polymer PDI, and it can be concluded that the suspension ATRP of MMA is sensitive to the monomer/initiator ratio in a batch reactor. Besides, an obvious decrease in the polymerization rate is reflected by the MMA concentration when the monomer/

initiator ratio increased from 50:1 to 300:1. Olga et al.[40] also investigated the effect of initial initiator mole fraction on the styrene/2-ethylhexyl acrylate emulsion copolymerization, and they also found similar results that the polymerization rate increases as the initiator concentration increases, while the initiator concentration does not seem to obviously affect the average particle size. With the increase in the initial initiator concentration, the consumption rate of MMA in the dispersed phase accelerates. An excellent final MMA conversion (>95%) is obtained when the monomer/initiator ratio is as high as 50:1. Figure 2B,C depicts the evolutions of polymer M_n and polymer PDI with respect to reaction time. The simulated result shows that M_n is extremely sensitive to the change of initiator concentration, and the low initiator concentration is conducive to prepare the high-molecular-weight polymer. From Figure 2B, it is apparent that the pace of M_n change accelerated as the monomer/initiator ratios rose. Furthermore, as can be seen in Figure 2C, the decreased initial initiator concentration slightly broadened the resulting

Makrials
Views
www.MaterialsViews.com

Macromol. React. Eng. **2016**, DOI: 10.1002/mren201500074
© 2016 WILEY-VCH Verlag GmbH & Co. KGaA, Weinheim

Macromolecular
Journals

7

Early View Publication; these are NOT the final page numbers, use DOI for citation !!

molecular weight distribution of the polymer products. Despite those, the PDI eventually levels at a value < 1.2, which indicates that the suspension ATRP system is still under control. The variation of M_n with monomer conversion under different monomer/initiator ratios is given in Figure 2D. The M_n increases almost linearly with monomer conversion, which further proves that the polymerization process is basically a controlled fashion.

4.2.2. The Effect of the Ratio of Water to Monomer

Compared with bulk or solution polymerization, suspension polymerization contains more than one phase. Although the polymerization takes place only within the dispersed phase because of the oil-soluble initiators, the aqueous phase does play an important role in heat transfer and monomer concentration distribution during the polymerization. Herein, we also simulate the effect of water/monomer (W/M) ratio on suspension ATRP of MMA. MMA is partially soluble in water, therefore the phase equilibrium of MMA is established between aqueous phase and dispersed phase. The monomer dissolved in the aqueous phase does not react until phase equilibrium forces it to transport to the dispersed phase to replenish monomer when the polymerization proceeds.[19] Thus, the W/M ratio will determine MMA concentration distribution in the two phases, and in turn affect the suspension polymerization and polymer products performance. Figure 3 displays the variation of the overall monomer conversion and PDI as a function of time when the W/M ratio ranges from 4:1 upto 1:1, which is applied in most commercial processes.[16] Here, the suspension polymerization will become a bulk polymerization when the W/M ratio approaches 0. It can be clearly seen from Figure 3 that the suspension and bulk polymerization monomer conversions become almost identical when the water to monomer ratio is smaller than

2. This is because the fraction of monomer in aqueous phase decreases with the increase of the volume fraction of dispersed phase. Furthermore, it is obvious that the rate of bulk polymerization is faster than that of suspension polymerization. However, both the final monomer conversion levels at a value >80% at the reaction time of 10 000 s or later. Although the W/M ratio has a significant effect on the monomer conversion and polymer M_n (data are not shown here because of the similar trend of M_n vs time as described in Section 4.2.1), the polymer PDI seems to be independent of the change of W/M ratio (see Figure 3B). It means that the monomer concentration distribution caused by phase separation has little influence on the molecular weight distribution of the polymer products. According to the work of Zhu et al.,[13] the PDI was significantly affected by the reversible equilibrium reaction in ATRP, namely, it is the activator or deactivator instead of monomer concentration that may have a strong influence on the PDI.

4.3. The Suspension ATRP Droplet/Particle Kinetics

The PBM suggested in this work is solved together with polymerization kinetic equations and constitutive equations, describing the physical properties of dispersed phase in MMA suspension polymerization. The kinetic, transport, and physical parameters, appearing in the PSD model, are employed in the simulations. A number of simulations were performed to investigate the effect of operating conditions on the dynamic behavior of droplet size that is determined by both breakage and coalescence rates over a wide range of conditions. Figures 4–6 illustrate the volume density function of the dispersed phase changes when the suspension polymerization proceeds and Figure 7 displays the effect of agitation speed on the Sauter mean diameter.

Figures 4 and 5 give the effect of breakage and coalescence phenomena on the time evolution of the PSD
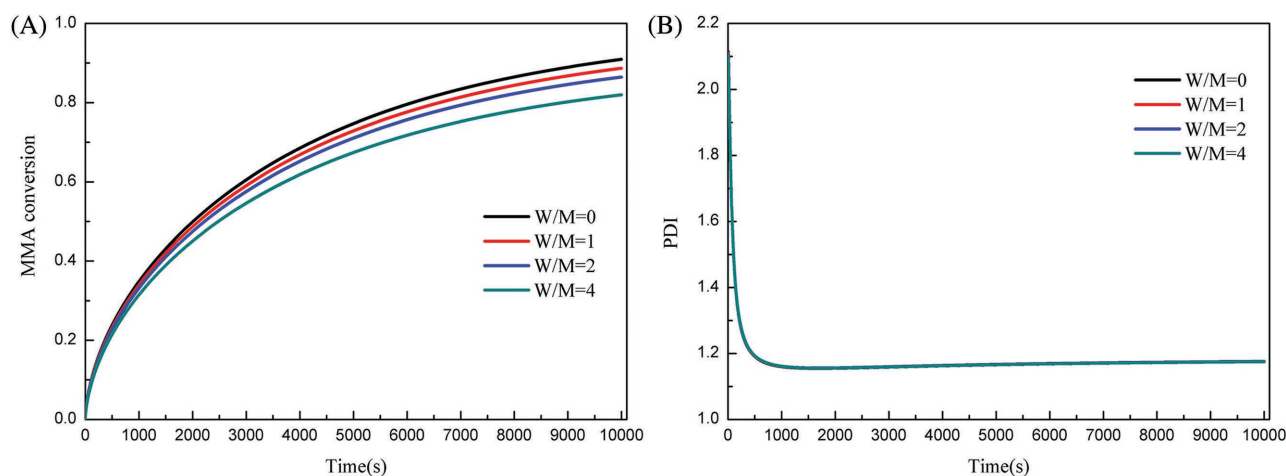

Figure 3. Simulation results of batch suspension ATRP process at three M/W ratios: A) monomer conversion (X_m) versus time, B) PDI versus time. MMA suspension polymerization at 90 °C and $[MMA]_o = 9.36$ mol L^{-1}; $[RX]_o = 0.047$ mol L^{-1}; $[CuCl]_o = 0.047$ mol L^{-1}; $[bpy]_o = 0.14$ mol L^{-1}.

Early View Publication; these are NOT the final page numbers, use DOI for citation !!

Modeling of the Methyl Methacrylate Atom Transfer Radical Suspension Polymerization Process: Polymerization . . .

Macromolecular
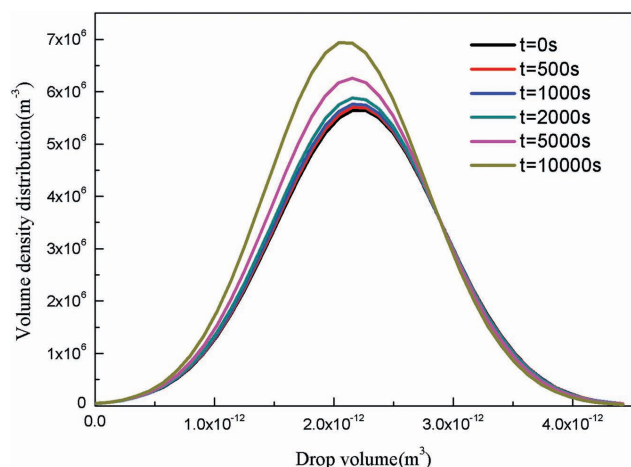Reaction Engineering

www.mre-journal.de

Figure 4. Effect of the breakage rate on the droplet volume density distribution at different time points.

in terms of the volume density function when the given average energy dissipation rate is 0.0382 W kg^{-1} (200 rpm). There shows a great difference for the volume number density at different instant points, which means that the breakage and coalescence plays an important role on the total PSD in suspension polymerization. In Figure 4, the simulated results show that as the droplets break, the total droplet number increases, while the droplet size decreases. On the contrary, the droplet size increases in the process of coalescence as shown in Figure 5. According to the mathematical model established in Section 2, the breakage rate is highly dependent on operating conditions, i.e., agitation speed, while the coalescence rate is influenced mainly by the dispersed phase physical properties, i.e., density and viscosity, which changes significantly in the process of suspension polymerization. Furthermore, it is well-known that the disperse-phase Sauter mean diameter will either decrease
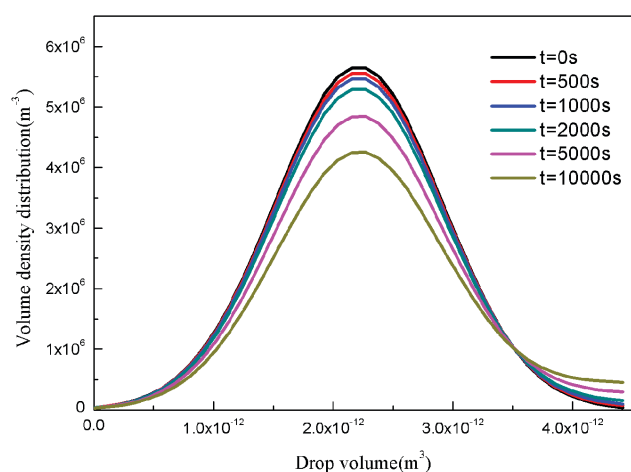
or increase when breakage or coalescence effect is dominated in the suspension polymerization.

In this study, the particle breakage and coalescence rates are mainly determined by mixing power per unit volume combined with tip shear rate of stirrer paddle. In other words, breakage and coalescence rates are dependent on both the operating parameters (i.e., agitation speed) and reactor structural parameters (i.e., type of stirrer paddle, installation location). The agitation speed, as one of the most important influence factors, can affect the average energy dissipation rate (ε) that is an important parameter in PBM (see Equations (26) and (27)). Therefore, only the effect of stirrer speed on the dynamic behavior of droplet size is studied herein when the reactor has been specified. Figure 6 displays the dispersed phase volume density function at different times with different agitation speeds of 200 rpm ($\varepsilon = 0.0382$ W kg^{-1}), 300 rpm ($\varepsilon = 0.1101$ W kg^{-1}), and 400 rpm ($\varepsilon = 0.2692$ W kg^{-1}). As can be seen in Figure 6, with the increase of agitation speed, the droplets volume density function changes observably. When the stirring rate is 200 rpm, the breakage rate and coalescence rate are approximately equal to each other and the total droplets volume density distribution seems to remain the same. Similar results can also be seen in Figure 7 that the droplet Sauter mean diameter remains unchanged under the low agitation speed ($N = 200$ rpm). When the agitation speed is as high as 400 rpm, however, a large number of small droplets are generated due to the breakage events (see Figure 6C). Figure 7 illustrates the influence of agitation speed on droplets diameter in details. At first, the Sauter mean diameter has a simple linear relation with time. What's more, there is a great difference in the droplets diameter under three different agitation speeds, which further proves the importance of agitation speed in suspension polymerization.

5. Conclusions

In this work, a comprehensive mathematical model was developed to describe the dynamic behavior of the batch suspension MMA ATRP. The suspension ATRP kinetic model, the thermodynamics equilibrium of the suspension system, and the rate of droplet breakage and coalescence were considered to investigate the suspension polymerization system. Open experimental data were applied to validate the above model. Based on the validated model, extensive simulations were performed to investigate the influences of the operating conditions on polymerization and particle kinetics. First, the monomer/initiator ratio has significant effect on monomer conversion, M_n and PDI. An excellent final MMA conversion (>95%) and PDI value (<1.2) are obtained when monomer/initiator ratio is as high as 50:1. In addition, when the water to monomer
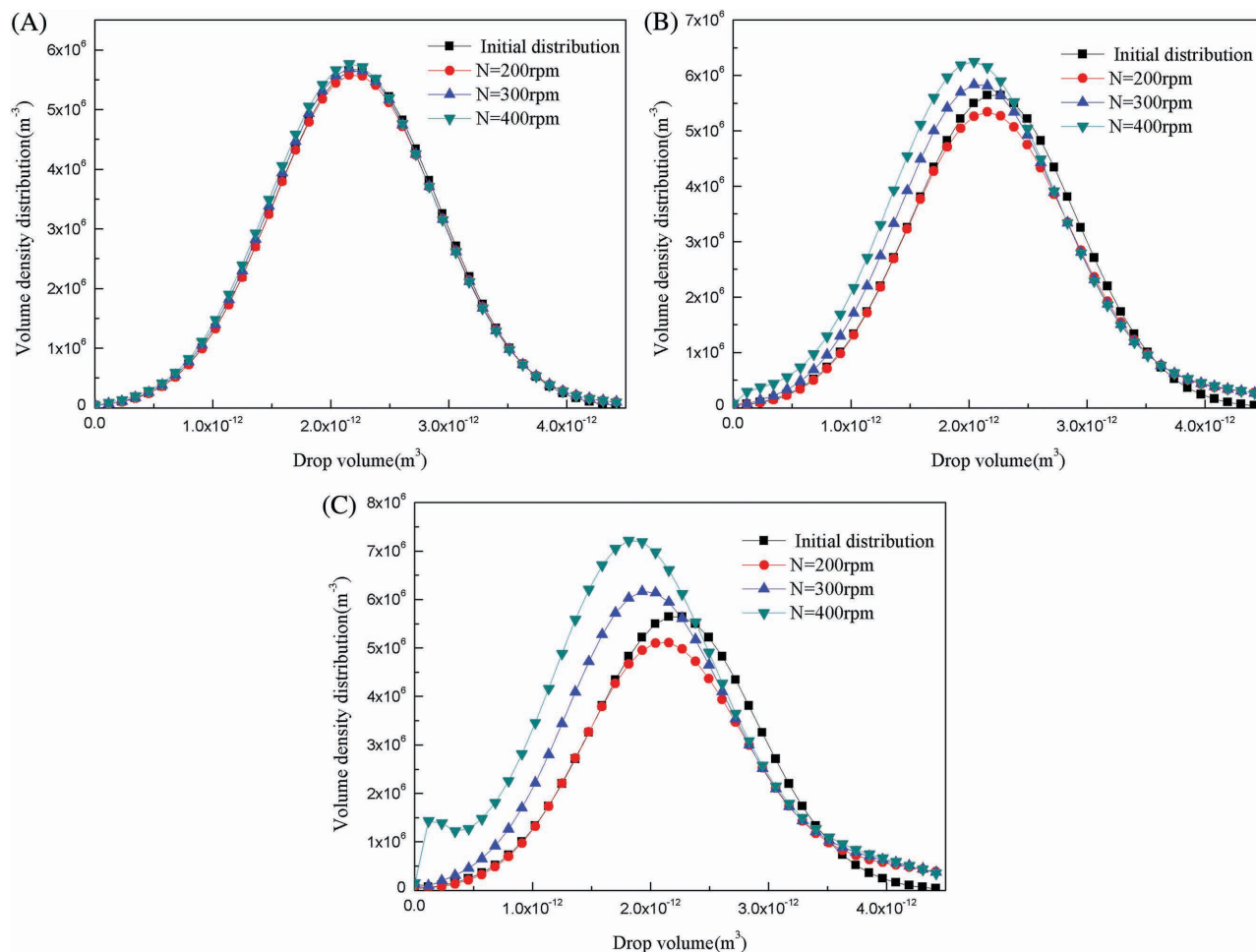

Figure 5. Effect of the coalescence rate on the droplet volume density distribution at different time points.

Early View Publication; these are NOT the final page numbers, use DOI for citation !!

Figure 6. Effect of the agitation speed on the droplet volume density distribution at different time points: A) *t* = 1000 s, B) *t* = 5000 s, C) *t* = 10 000 s.

ratio is smaller than 2, the monomer conversions of suspension and bulk polymerization become almost equal to each other. For particle kinetics, the effect of breakage and
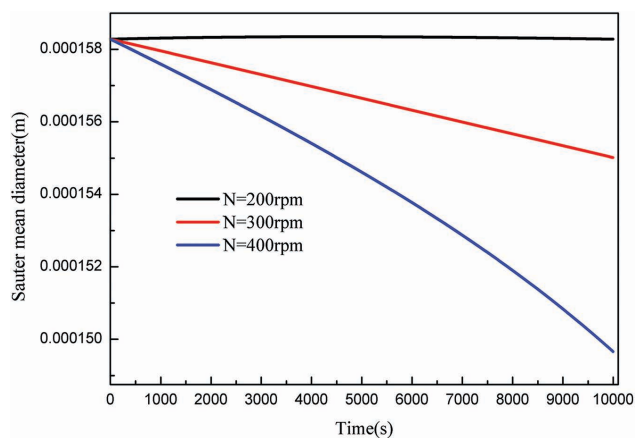

Figure 7. Effect of the agitation speed on the Sauter mean diameter during the whole polymerization.

coalescence event on the time evolution of the volume density function were obtained respectively, attention was also paid to the effect of agitation speed on the droplets volume density distribution and Sauter mean diameter. When the stirring rate is 200 rpm, the breakage rate and coalescence are comparable and the total droplets volume density distribution seems to remain the same. When the agitation speed is as high as 400 rpm, however, a large number of small droplets are generated due to the breakage events.

As a whole, the established comprehensive model could better capture the whole suspension polymerization information including the time evolution of conversion, M_n, PDI, droplet volume density distribution, and Sauter mean diameter. It is believed that the current model may contribute to a more rational design of suspension polymerization reactors. Recently, much attention was paid to the CFD to provide detailed flow fields information in polymerization reactor. Therefore, the more realistic CFD model based on the current simulation results will be developed in our future work.

www.MaterialsViews.com

Early View Publication; these are NOT the final page numbers, use DOI for citation !!

Modeling of the Methyl Methacrylate Atom Transfer Radical Suspension Polymerization Process: Polymerization . . .

Macromolecular
Reaction Engineering

www.mre-journal.de

[1] J. S. Wang, K. Matyjaszewski, *Macromolecules* **1995**, *28*, 7901.
[2] M. Kato, M. Kamigaito, M. Sawamoto, T. Higashimura, *Macromolecules* **1995**, *28*, 1721.
[3] K. Matyjaszewski, J. Xia, *Chem. Rev.* **2001**, *101*, 866.
[4] N. V. Tsarevsky, K. Matyjaszewski, *Chem. Rev.* **2007**, *107*, 2270.
[5] K. Matyjaszewski, *Macromolecules* **2012**, *45*, 4015.
[6] K. Matyjaszewski, N. V. Tsarevsky, *J. Amer. Chem. Soc.* **2014**, *136*, 6513.
[7] M. Destarac, *Macromol. React. Eng.* **2010**, *4*, 165.
[8] J. L. Wang, T. Grimaud, K. Matyjaszewski, *Macromolecules* **1997**, *30*, 6507.
[9] E. Rusen, A. Mocanu, *Colloid Polym. Sci.* **2013**, *291*, 2253
[10] S. Jousset, J. Qiu, *Macromolecules* **2001**, *34*, 6641.
[11] C. Granel, P. Dubois, R. Jérôme, P. Eyssié, *Macromolecules* **1996**, *29*, 8576.
[12] T. Nishikawa, M. Kamigaito, M. Sawamoto, *Macromolecules* **1999**, *32*, 2204.
[13] C. Zhu, S. Fei, Z. Min, J. Jian, *Polymer* **2004**, *45*, 1141.
[14] J. Cao, L. Zhang, X. Jiang, C. Tian, X. Zhao, Q. Ke, X. Pan, Z. Cheng, X. Zhu, *Macromol. Rapid Commun.* **2013**, *34*, 1747.
[15] Z. Chen, W. Pauer, H. U. Moritz, J. Prüss, H. J. Warnecke, *Chem. Eng. Technol.* **1999**, *22*, 609.
[16] G. Kalfas, H. Yuan, W. H. Ray, *Ind. Eng. Chem. Res.* **1993**, *32*, 1831.
[17] S. X. Zhang, W. H. Ray, *Ind. Eng. Chem. Res.* **1997**, *36*, 1310.
[18] T. W. Taylor, K. H. Reichert, *J. Appl. Polym. Sci.* **1985**, *30*, 227.
[19] G. Kalfas, W. H. Ray, *Ind. Eng. Chem. Res.* **1993**, *32*, 1822.
[20] F. M. Silva, E. L. Lima, J. C. Pinto, *Ind. Eng. Chem. Res.* **2004**, *43*, 7324.
[21] J. Wieme, T. D. Roo, G. B. Marin, G. J. Heynderickx, *Ind. Eng. Chem. Res.* **2007**, *46*, 1179.
[22] E. Vivaldo-Lima, P. E. Wood, A. E. Hamielec, A. Penlidis, *Ind. Eng. Chem. Res.* **1997**, *36*, 939.
[23] D. Maggioris, A. Goulas, A. H. Alexopoulos, E. G. Chatzi, C. Kiparissides, *Chem. Eng. Sci.* **2000**, *55*, 4611.
[24] C. Kotoulas, C. Kiparissides, *Chem. Eng. Sci.* **2006**, *61*, 332.
[25] E. S. Nogueira, J. C. Pinto, A. S. Vianna, *Can. J. Chem. Eng.* **2012**, *90*, 983.
[26] Á. Bárkányi, S. Németh, B. G. Lakatos, *Comput. Chem. Eng.* **2013**, *59*, 211.
[27] S. P. Zhu, *Macromol. Theory Simul.* **1999**, *8*, 29.
[28] S. P. Zhu, *J. Polym. Sci. Pol. Phys.* **1999**, *37*, 2692.
[29] R. Wang, Y. W. Luo, B. G. Li, X. Y. Sun, S. P Zhu, *Macromol. Theory Simul.* **2006**, *15*, 356.
[30] W. Wang, Y. N. Zhou, Z. H. Luo, *Ind. Eng. Chem. Res.* **2014**, *53*, 11873.
[31] W. Wei, Y. N. Zhou, Z. H. Luo, *Macromol. React. Eng.* **2015**. *9*, 418.
[32] J. Ugelstad, P. C. Mórk, K. H. Kaggerud, T. Ellingsen, A. Berge, *Adv. Colloid Interface Sci.* **1980**, *13*, 101.
[33] C. A. Coulaloglou, L. L. Tavlarides, *Chem. Eng. Sci.* **1977**, *32*, 1289.
[34] Y. N. Zhou, J. J. Li, Z. H. Luo, *J. Polymer Sci., Part A: Polymer. Chem.* **2012**, *15*, 3052.
[35] E. V. Lima, R. G. Pérez, O. J. C. Briones, *J. Mex. Chem. Soc.* **2003**, *1*, 22.
[36] Y. N. Zhou, Z. H. Luo, *Macromolecules* **2014**, *18*, 6218.
[37] J. Brandrup, E. H. Immergut, E. A. Grulke, *Polymer Handbook Edition*, New York: John Wlley & Sons, **1999**.
[38] K. K. Singh, S. M. Mahajani, K. T. Shenoy, S. K. Ghosh, *Hydrometallurgy* **2008**, *90*, 121.
[39] B. Brooks, *Chem. Eng. Technol.* **2010**, *33*, 1737.
[40] K. Olga, P. Prokopis, C. E. Frantzikinakis, K. Costas, *Macromol. Chem. Phys.* **2003**, *204*, 983.

Early View Publication; these are NOT the final page numbers, use DOI for citation !!